Chemical Science

ROYAL SOCIETY OF CHEMISTRY

EDGE ARTICLE

View Article Online
View Journal | View Issue

Cite this: *Chem. Sci.*, 2023, **14**, 5405

All publication charges for this article have been paid for by the Royal Society of Chemistry

Rational synthesis of elusive organic–inorganic hybrid metal-oxo clusters: formation and post-functionalization of hexavanadates†

David E. Salazar Marcano, ‡[a] Givi Kalandia, ‡[a] Mhamad Aly Moussawi, [a] Kristof Van Hecke [b] and Tatjana N. Parac-Vogt *[a]

Paving the way towards new functional materials relies increasingly on the challenging task of forming organic–inorganic hybrid compounds. In that regard, discrete atomically-precise metal-oxo nanoclusters have received increasing attention due to the wide range of organic moieties that can be grafted onto them through functionalization reactions. The Lindqvist hexavanadate family of clusters, such as $[V_6O_{13}\{(OCH_2)_3C\text{-}R\}_2]^{2-}$ (V_6-R), is particularly interesting due to the magnetic, redox, and catalytic properties of these clusters. However, compared to other metal-oxo cluster types, V_6-R clusters have been less extensively explored, which is mainly due to poorly understood synthetic challenges and the limited number of viable post-functionalization strategies. In this work, we present an in-depth investigation of the factors that influence the formation of hybrid hexavanadates (V_6-R HPOMs) and leverage this knowledge to develop $[V_6O_{13}\{(OCH_2)_3CNHCOCH_2Cl\}_2]^{2-}$ (**V_6-Cl**) as a new and tunable platform for the facile formation of discrete hybrid structures based on metal-oxo clusters in relatively high yields. Moreover, we showcase the versatility of the **V_6-Cl** platform through its post-functionalization *via* nucleophilic substitution with various carboxylic acids of differing complexity and with functionalities that are relevant in multiple disciplines, such as supramolecular chemistry and biochemistry. Hence, **V_6-Cl** was shown to be a straightforward and versatile starting point for the formation of functional supramolecular structures or other hybrid materials, thereby enabling their exploration in various fields.

Received 3rd January 2023
Accepted 22nd April 2023

DOI: 10.1039/d3sc00038a

rsc.li/chemical-science

Introduction

Over time, the ability to synthesize increasingly complex chemical structures has begun to blur the line between organic and inorganic materials. The formation of organic–inorganic hybrid materials that synergistically combine the properties of both organic and inorganic components has attracted attention especially for the development of functional materials.[1] Therefore, in recent years, metal-oxo clusters have emerged as valuable building-blocks for the formation of a variety of discrete organic–inorganic hybrid structures. Of the multiple possible hybrid structures, hybrid polyoxometalates (HPOMs) have particularly garnered significant interest due to their applications in catalysis, materials science, energy storage, medicine, and supramolecular chemistry.[2–8] HPOMs are a subclass of a diverse family of discrete anionic metal-oxo clusters, commonly known as polyoxometalates (POMs), that can be covalently grafted with a wide range of organic molecules through the replacement of a metal centre by organophosphorus, organosilicon, organogermanium or organotin species or through replacement of the oxo ligands by alkoxides or amines.[2,9] Such functionalization of metal-oxo clusters with various moieties has already proven beneficial, for example, in enhancing their catalytic activity and efficiency.[10–12] Additionally, organic derivatization has been recently demonstrated as a valuable strategy for addressing important challenges in renewable energy and energy storage.[13,14] Moreover, these hybrid clusters can be regarded as analogues for MO_x hybrid materials such as Metal Organic Frameworks (MOFs) and functionalized metal oxide nanoparticles or surfaces, due to similarities in their structure and electronic delocalization.[15] In fact, several MOFs based on HPOM building units have been reported showing the close connection between such hybrid frameworks and HPOMs.[16–19] However, the discrete atomically-precise structures of HPOMs and their solubility in many different solvents make them easier to study, thereby providing insights about metal-oxo based materials in general. Therefore, the synthetic challenges faced in the formation of MO_x hybrid materials are more easily tackled at the scale of HPOMs. Hence,

[a]*Department of Chemistry, KU Leuven, Celestijnenlaan 200F, 3001 Leuven, Belgium. E-mail: tatjana.vogt@kuleuven.be*

[b]*XStruct, Department of Chemistry, Ghent University, Krijgslaan 281, S-3, 9000 Ghent, Belgium*

† Electronic supplementary information (ESI) available. CCDC 2217991 and 2217992. For ESI and crystallographic data in CIF or other electronic format see DOI: https://doi.org/10.1039/d3sc00038a

‡ Authors contributed equally to this work.

the synthesis of more complex novel HPOMs is likely to drive progress in many different fields.

Although hybrid metal-oxo clusters have been attracting increasing attention in recent years, the factors that influence their formation in solution are still not well understood. As a result, there is a rather limited selection of HPOMs that can be easily functionalized with various organic moieties. This is particularly the case for the Lindqvist hexavanadate HPOMs, such as $[V_6O_{13}\{(OCH_2)_3C\text{-}R\}_2]^{2-}$ (V_6-R), which due to their interesting chemical and redox properties have been investigated in several fields including catalysis,[10,15] memory devices,[20] energy conversion/storage,[21] supramolecular self-assembly and host–guest chemistry, among others.[22,23] Moreover, these hexavanadate HPOMs have a great structural versatility, since they can be mono-, bis-, tris- or tetra-functionalized with triol ligands, depending on the composition and oxidation state of the metal centres.[24] However, despite V_6-R HPOMs being one of the first examples of HPOMs to be reported,[25] their synthesis and post-functionalization remain significantly less explored compared to other metal-oxo cluster types.[24,27,28] The relatively limited literature available on V_6-R HPOMs is likely due to the poor yields often obtained during their synthesis and the scarce number of V_6-R HPOMs that can be easily derivatized with a wide range of organic species. Hence, elucidating the formation mechanism of such clusters is essential to address the issues typically encountered during their synthesis.

In general, the synthesis of metal-oxo hybrids with complex organic moieties attached onto the inorganic core is often achieved by starting from a relatively simple building unit with a reactive terminal group that can then be modified through a post-functionalization reaction.[27] Therefore, $[V_6O_{13}\{(OCH_2)_3CCH_2OH\}_2]^{2-}$ (V_6-OH), which can be easily obtained from decavanadate ($[H_3V_{10}O_{28}]^{3-}$; V_{10}) and pentaerythritol ($(HOCH_2)_3CCH_2OH$),[29,30] is typically used for forming more complex V_6-R HPOMs with various organic moieties through esterification reactions with carboxylic acids and acid anhydrides, but it is not reactive towards many substrates (Scheme 1).[31,32] Alternatively, $[V_6O_{13}\{(OCH_2)_3CNH_2\}_2]^{2-}$ (V_6-NH_2) can be used as a post-functionalization platform with a more reactive amine terminal group. However, its synthesis from V_{10} and tris(hydroxymethyl)aminomethane ($(HOCH_2)_3CNH_2$; Tris-NH_2) typically results in very low yields (Scheme 1),[22,33,34] in contrast to other metal-oxo clusters that have been successfully functionalized with Tris-NH_2.[26,35] Due to this limitation, pre-functionalization of Tris-NH_2 is sometimes used for the direct formation of V_6-R HPOMs, but this also often results in relatively low yields.[28] Consequently, there is a need for post-functionalization platforms that can be employed to incorporate various organic functionalities onto V_6-R HPOMs in high yields, thereby driving the formation of new hybrid materials and expanding their potential applications. To achieve this goal, a deeper understanding of the factors that affect the synthesis and modification of these hybrid metal-oxo clusters is still necessary. Hence, by investigating the key factors in the synthesis of V_6-R HPOMs, a novel post-functionalization platform was developed. Moreover, this new HPOM was functionalized with multiple carboxylic acids of varying complexity to demonstrate the versatility of this platform in making the formation of hybrid polyoxovanadates more accessible compared to existing platforms.

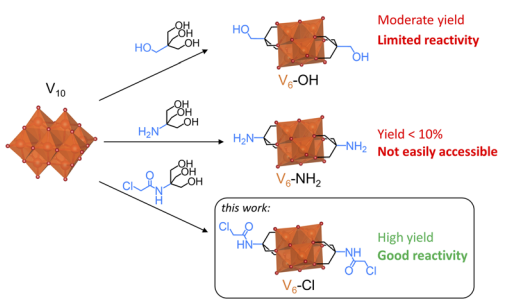

Scheme 1 Synthesis of hexavanadate post-functionalization platforms starting from V_{10} and triol ligands with reactive terminal groups.

Results and discussion

The low yields often obtained in the synthesis of V_6-R HPOMs are typically attributed to the ease of reduction of the V^{5+} centres.[22,33,34] However, to the extent of our knowledge, this has not been experimentally confirmed. Nevertheless, previously reported literature procedures suggest that the solvent and the nature of the functional groups on the triol ligand have a significant influence on the outcome of the reaction.[34,36,37] For example, literature reports show that V_6-OH can be easily synthesized in acetonitrile (ACN) and water while V_6-NH_2 can only be obtained directly in dimethylacetamide (DMA) and even in DMA the yield is typically less than 10% unless protecting groups are used.[22,29,30,33,34] Therefore, in order to understand what happens in solution during the synthesis of V_6-R HPOMs, we set out to study the reactions between V_{10} and different triol ligands by multinuclear NMR, IR and UV-vis-NIR spectroscopy as well as ESI-MS. Furthermore, the reaction of V_{10} with $(HOCH_2)_3CNHCOCH_2Cl$ (Tris-Cl) was investigated in detail, since this triol ligand can be easily synthesized in high yields at the gram-scale and its highly electrophilic chloroacetamide functionality can be exploited for nucleophilic substitution. As a result, the Tris-Cl ligand can be leveraged for post-functionalization with a wide variety of carboxylic acids, amines and thiols, as has been previously demonstrated by our group with other hybrid metal-oxo clusters.[38–40] Moreover, the high electrophilicity of the chloroacetamide carbon, and the S_N2 mechanism favoured under polar aprotic conditions, allow for easier substitution reactions with relatively bulky or less nucleophilic substrates than with V_6-OH and its derivatives. Additionally, the insights gained from following the reaction of V_{10} with various triol ligands were used to optimize the procedure for the synthesis of $TBA_2[V_6O_{13}\{(OCH_2)_3CNHCOCH_2Cl\}_2]$ (**V_6-Cl**) as a novel post-functionalization platform formed from Tris-Cl and V_{10} (Scheme 1).

Elucidating the impact of ligand functionalities

Following changes in the speciation of reaction mixtures of V_{10} in the absence or in the presence of three triol ligands by

multinuclear NMR, IR, UV-vis-NIR and ESI-MS gave distinct results depending on the triol ligand: $(HOCH_2)_3CCH_3$ (Tris-CH_3), Tris-NH_2, or Tris-Cl. This demonstrates the important role of the ligands and the nature of their terminal group as critical factors in determining the outcome of the reaction (Scheme 2). Although Tris-CH_3 and Tris-NH_2 have very similar structures, simply switching the methyl group for an amine had a major effect on the speciation of vanadates in solution. With Tris-CH_3, the desired hexavanadate structure, $[V_6O_{13}\{(OCH_2)_3CCH_3\}_2]^{2-}$ (V_6-CH_3), was observed to gradually form over time from the appearance of characteristic peaks in NMR and ESI-MS spectra while the peaks due to V_{10} disappeared (Fig. S1, S3, S14 and Table S6†).[29,41] In contrast, when V_{10} was reacted with Tris-NH_2 several peaks appeared in the ^{51}V NMR spectrum within 0.5 h of heating (Fig. S1†), indicating that multiple vanadate species formed, with the main species being $[V_{12}O_{32}]^{4-}$ (V_{12}) and $[V_{13}O_{34}]^{3-}$ (V_{13}).[42,43]

The formation of V_{12} and V_{13} in the presence of Tris-NH_2 may be due to the poor solubility of Tris-NH_2 in ACN (Table S2†), especially in comparison with Tris-CH_3, since the conversion of V_{10} into V_{12} and V_{13} was also observed when V_{10} was heated at 80 °C on its own in ACN (Scheme 2 and Fig. S1, S2†). Furthermore, V_{12} eventually became the main species in solution based on ^{51}V NMR (Fig. S1†) and on negative mode ESI-MS (Fig. S14 and Table S5†). Similarly, the IR spectrum of V_{10} alone after heating gave rise to characteristic peaks of V_{12} between 1200 and 400 cm^{-1} that were also observed after heating with Tris-NH_2 (Fig. S11†).[43] Therefore, it is likely that in the reaction with Tris-NH_2, only a small amount of the triol was present in solution at any given time, which reacted with V_{10} to form other vanadate species that gave rise to several peaks around 5 ppm in the ^{1}H NMR spectrum (Fig. S4†) along with additional peaks in the ^{51}V NMR spectrum. These are likely caused by Tris-NH_2 reacting with V_{10} through both the –OH and –NH_2 groups, since reacting with just the –OH groups would result in the formation of the desired hexavanadate as observed for Tris-CH_3. In addition, over time, the peaks observed by ^{51}V NMR gradually disappeared, except for a peak at −498 ppm, which may correspond to V_6-NH_2. However, this peak is relatively weak. Therefore, together with the IR and ESI-MS spectra (Fig. S14 and Table S7†), this suggests that V_6-NH_2 is only present in low concentration after 120 h.

In contrast, the reaction of V_{10} with Tris-Cl did not give rise to observable peaks (Fig. S1†) corresponding to V_{12} and V_{13} in the ^{51}V NMR spectra, which may be due to the higher solubility of Tris-Cl in ACN with respect to Tris-NH_2 (Table S2†). Instead, two broad peaks were observed to appear at −228 and −294 ppm in the ^{51}V NMR spectrum of the reaction mixture (Fig. S1†), which correspond to V environments that are more deshielded than expected for fully oxidized vanadates with oxo or alkoxo ligands.[44] Hence, these new peaks may be due to paramagnetic shifting of V^{5+} centres in mixed valence vanadates or due to coordination of the ligand to V^{5+} centres through nitrogen.[44] Furthermore, as with Tris-NH_2, the reactions of vanadate species with the Tris-Cl ligand resulted in the gradual disappearance of most peaks observed by ^{51}V NMR except for two weak peaks: one at −364 ppm, belonging to $VO_2Cl_2^-$ formed through the decomposition of Tris-Cl, and another at around −498 ppm, likely due to **V_6-Cl** present in low concentration (Fig. S1†).[44] Likewise, the presence of **V_6-Cl** in low concentration together with side-products after 120 h could be observed by ^{1}H NMR (Fig. S5†). These changes observed by NMR can be attributed to reduction of V^{5+} centres to form mixed valence species.

The formation of mixed valence vanadates in the presence of Tris-NH_2 or Tris-Cl is confirmed by the observed change in colour of the solutions over time from orange/yellow (typical of V^{5+}) to dark green, which is indicative of the reduction of some V^{5+} centres to form a mixture of V^{5+} and V^{4+}.[16,45] This was confirmed by the appearance of a characteristic peak in the absorbance spectrum at around 900 nm due to an Intervalence Charge Transfer (IVCT) between V^{4+} and V^{5+} (Fig. 1 and Tables S3, S4†). Since the appearance of this IVCT broad peak is not as noticeable for V_{10} alone or in the presence of Tris-CH_3 (Fig. 1 and S10†), the reduction of V^{5+} is most likely due to N–H···O–V interactions. Such N–H···O–V interactions have indeed been recently reported in crystal structures of V_{10} with Tris-NH_2.[45] Furthermore, a similar reduction process has been proposed to result in the photoinduced reduction of alkylammonium salts of molybdates and is likely responsible for the reduction of NH_4VO_3 by the NH_4^+ counterion during its thermal decomposition.[46–48]

Reduction of V^{5+} may take place through the transfer of the N–H proton onto the oxo ligands of V_{10} or other vanadates that may form in solution.[34] This likely occurs through a similar process to the formation of mixed valence or fully reduced V_6-R HPOMs with protonated μ_2-O ligands in the presence of hydrazine derivatives and organic acids, which has been reported to involve a proton-coupled electron transfer (PCET).[15,29,34,49] However, since the structure of the side-products could not be identified, the exact nature of the reduction mechanism could not be unambiguously determined. Nevertheless, it can be concluded that the main product for the reaction of Tris-Cl and Tris-NH_2 with V_{10} in ACN is not the desired V_6-R HPOMs because of side-reactions giving rise to reduced vanadate species. This is evidenced by ESI-MS and IR spectroscopy (Fig. S11, S12, S14 and Tables S7, S8†), which after 120 h at 80 °C mainly showed peaks that did not correspond to the desired hexavanadates. Moreover, this indicates that the yield of V_6-R HPOMs depends highly on how the speciation of

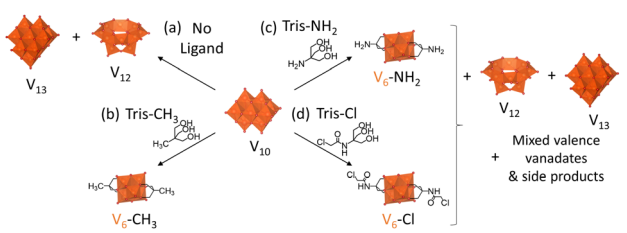

Scheme 2 Speciation of V_{10} in ACN after heating at 80 °C for 0–24 h: (a) alone or with (b) Tris-CH_3, (c) Tris-NH_2 or (d) Tris-Cl.

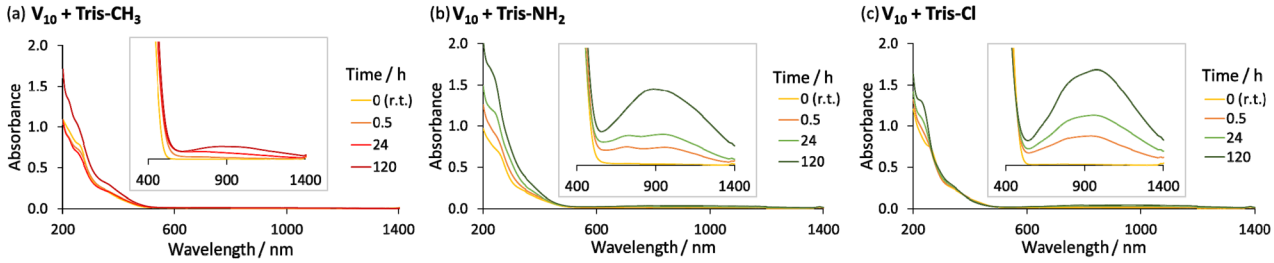

Fig. 1 UV-vis-NIR absorbance spectra of V_{10} with (a) Tris-CH_3, (b) Tris-NH_2, or (c) Tris-Cl after 0 h at room temperature (r.t.) and after 0.5, 24, and 120 h at 80 °C, with the broad IVCT peak shown in the insert.

vanadates is affected by the ligand's availability in solution and the reactivity of its functional groups.

Investigating the role of the solvent

Since DMA has also been previously reported as a solvent in optimized procedures,[36,37] in this work the impact of the solvent on the formation of **V_6-Cl** was investigated further. In doing so, the use of DMA as the solvent for the synthesis of **V_6-Cl** was determined to be crucial for obtaining the product in relatively high yields, since the attempted synthesis in ACN or in water, following the typical procedures used for the formation of hexavanadates, resulted in many side products, which hindered the isolation of **V_6-Cl**.[29,30] The differences in the reaction of V_{10} with Tris-Cl in ACN *vs.* in DMA can be seen from the ^{1}H and ^{51}V NMR spectra of aliquots obtained over 20 h, which showed more intense peaks corresponding to **V_6-Cl** when the reaction was conducted in DMA (Fig. 2 and S7†). This means that the formation of **V_6-Cl** is more favourable in DMA, which may be in part due to the higher solubility of Tris-Cl in this solvent (Table S2†). Furthermore, when V_{10} is heated at 80 °C in DMA without any triol ligands, the speciation is quite different from that in ACN (Fig. S6†). While the V_{12} structure is highly favoured in ACN, V_{13} is the main species in DMA along with multiple other vanadate species of lower nuclearity, ranging from V_1 to V_5, which gradually disappear over time.[44] This suggests that the vanadate structures are more labile and prone to interconversion in DMA than in ACN, generating a dynamic library of interconverting vanadate building blocks, which may also facilitate the formation of hexavanadates in DMA.

It was also observed that changing the solvent had an impact on the ability of V^{5+} centres to be reduced. The cyclic voltammogram (CV) of **V_6-Cl** in either ACN or DMA (Fig. 3(a)) shows a similar reversible reduction/oxidation wave due to the V^{5+}/V^{4+} redox couple in both solvents, but the half-wave potential ($E_{1/2}$) is more negative in DMA compared to in ACN: −1.01 and −0.80 V *vs.* Fc/Fc^+, respectively.[50] Similarly, V_6-CH_3 gives rise to reversible reduction/oxidation waves with $E_{1/2}$ of −1.07 and −0.92 V *vs.* Fc/Fc^+ in DMA and in ACN, respectively (Fig. S18†). Hence, the reduction of V^{5+} occurs more easily in ACN. This solvent-induced shift in $E_{1/2}$ is likely due to the higher Lewis acidity of ACN, as reflected by the Gutmann acceptor number of ACN (18.9) being higher than that of DMA (13.6).[51] Furthermore, these results are in agreement with the previously reported trend in the redox potential of tungstate POMs in different solvents.[52,53] However, the solvent-induced shift in $E_{1/2}$ is greater for **V_6-Cl** (215 mV) than for V_6-CH_3 (150 mV), which may be linked to the N–H···O–V interactions observed in the crystal structure obtained by crystallization in ACN (Fig. 3(c)) since protonation of oxo ligands in the vanadate clusters has been

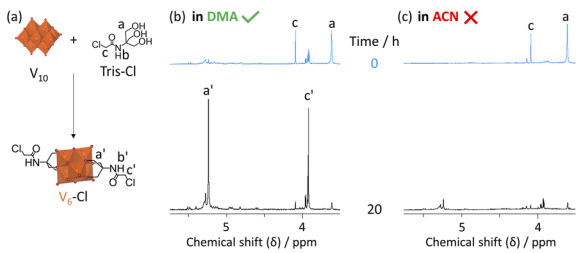

Fig. 2 (a) Synthesis of **V_6-Cl** from V_{10} and Tris-Cl along with the corresponding ^{1}H NMR spectra of aliquots of the reaction mixture after heating at 80 °C for 0 and 20 h in (b) DMA or (c) ACN. All spectra were acquired for solutions in ACN-d_3 of the precipitate formed by addition of excess of diethyl ether to the aliquot.

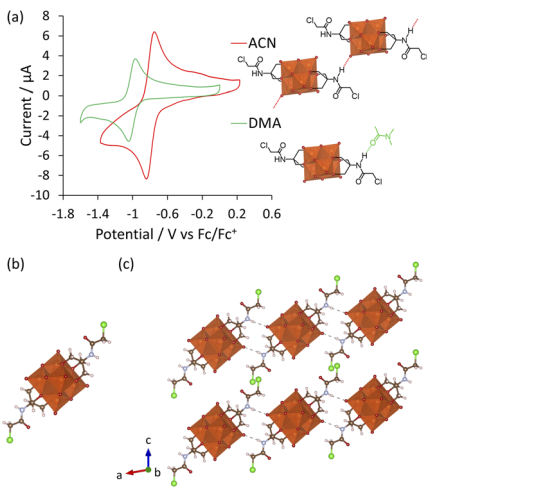

Fig. 3 (a) CV of 0.5 mM **V_6-Cl** in ACN *vs.* in DMA with 0.1 M TBA-PF_6 as the electrolyte (100 mV s^{-1}). (b) Structural representation of **V_6-Cl** viewed along the crystallographic b axis and (c) crystal packing of **V_6-Cl** into a 1D H-bond network (H-bond distances shown as dashed grey lines). The counter ions were omitted from the structural representations for clarity. Hydrogen in white, carbon in brown, nitrogen in light blue, oxygen in red, chlorine in green and vanadium in orange.

shown to result in shifts towards lower potentials.[29] In contrast, the crystal structure of a similar V_6-R HPOM with an amide group obtained by Bamba *et al.* in DMA shows that DMA forms H-bonding interactions between its C=O group and the –NH group of the ligand, thereby preventing N–H···O–V interactions from occurring.[54] Therefore, reduction of V^{5+} induced by transfer of the proton from the ligand is less likely to occur in DMA than in ACN, making it overall a more suitable solvent.

Isolation and characterisation of V_6-Cl

Through optimization of the synthesis and purification procedures based on the insights obtained by following the reactions of the triols, it was possible to obtain **V_6-Cl** directly from V_{10} and Tris-Cl in relatively high yield after reacting in DMA at 80 °C under an argon atmosphere for 5 days. However, despite the synthesis of **V_6-Cl** being more successful in DMA than in ACN, some side reactions resulting in the reduction of V^{5+} do still occur, as evidenced by the observed colour change of the solution. This is due to the formation of a mixture of the desired fully oxidized **V_6-Cl** and mixed valence **V_6-Cl**. Nevertheless, through the removal of DMA by rotary evaporation and the addition of a minimal amount of ACN, the mixed valence species were preferentially dissolved, forming a green solution, and the pure fully oxidized **V_6-Cl** could be separated by centrifugation as an orange crystalline solid. Furthermore, the mixed valence **V_6-Cl** in the green supernatant was successfully oxidized into the desired fully oxidized **V_6-Cl** by the addition of 35 wt% H_2O_2. Additionally, washing with water as well as re-precipitation with ACN/Et_2O and MeOH/Et_2O allowed for further purification of the re-oxidized sample as described in the SI. Moreover, through this re-oxidation and purification procedure the yield was increased to 61%.

The composition of **V_6-Cl** in high purity in the combination of the first fully oxidized sample and the re-oxidized sample was confirmed by ESI-MS, NMR, IR, and elemental analysis (Fig. 4). ESI-MS gave a peak at m/z = 1145.8 in negative mode, corresponding to **V_6-Cl** with only one TBA counter cation ([**V_6-Cl** + TBA]$^-$; calcd. m/z = 1145.3) while in positive mode it gave a peak at m/z = 1630.1 that can be attributed to the POM with three TBA counter ions ([**V_6-Cl** + 3TBA]$^+$; calcd. m/z = 1630.2). Furthermore, ^{1}H NMR showed a downfield shift from 3.57 ppm for Tris-Cl to 5.11 ppm for **V_6-Cl**, corresponding to the –CH_2O– group of the triol ligand becoming grafted onto the V_6 POM core, while ^{51}V NMR gave a single peak at −494 ppm that is characteristic of *trans*-functionalized hexavanadates.[34,54] Furthermore, the peaks in the IR spectrum in the range 700–1000 cm^{-1} are characteristic of ν V=O and ν V–O–V vibrations of the V_6 POM core, while the peaks at 1114 and 1063 cm^{-1} due to ν C-O vibrations confirm the successful attachment of the triol ligands.[30,55] The exact structure of **V_6-Cl** was further confirmed by single crystal X-ray diffraction (SC-XRD). **V_6-Cl** crystallized in the triclinic space group *P*1 with half of one POM and one TBA cation in the asymmetric unit. The obtained crystal structure (Fig. 3(b)) shows a classical Lindqvist structure composed of six edge sharing {VO_6} octahedra in an octahedral arrangement. Moreover, two Tris-Cl moieties are attached on

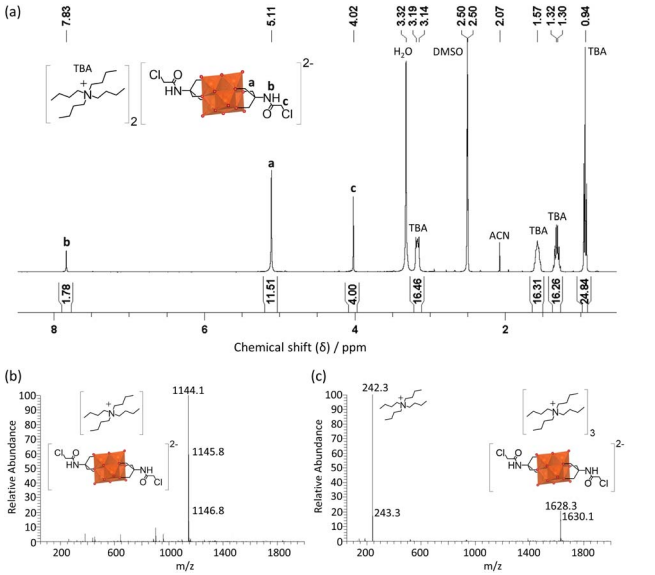

Fig. 4 (a) ^{1}H NMR spectrum of **V_6-Cl** in DMSO-d_6 as well as (b) negative mode and (c) positive mode ESI-MS spectra of **V_6-Cl** in ACN.

opposite faces of the V_6 POM core *via* three double-bridged oxygens (μ_2-O) each. In addition, **V_6-Cl** was observed to form a 1D H-bond network due to H-bonding interactions between the –NH group of the amide and a terminal oxygen of the V_6 POM core with N···O distances of 2.91 Å (Fig. 3(c)). Overall, the crystal structure together with the complementary spectroscopic techniques unambiguously confirm the formation of this novel post-functionalization platform.

Post-functionalization of V_6-Cl

The potential of **V_6-Cl** as a valuable post-functionalization platform was evaluated *via* nucleophilic substitution reactions with different carboxylic acids: valeric acid, phenylacetic acid, adamantanecarboxylic acid, and biotin (Scheme 3). These carboxylic acids were selected to showcase the applicability of this post-functionalization strategy to yield compounds with widely different functionalities. Furthermore, functionalities that are of interest in supramolecular chemistry were chosen since HPOMs have been shown to produce new dynamic supramolecular structures that often result in enhanced properties.[8] Consequently, four novel V_6-R HPOMs were synthesized from **V_6-Cl** and the aforementioned carboxylic acids: $TBA_2[V_6O_{13}\{(OCH_2)_3CNHCOCH_2\text{-}R\}_2]$ where R = –$OOC(CH_2)_3CH_3$ (**V_6-Val**), –$OOCCH_2C_6H_5$ (**V_6-Ph**), –$OOCC_{10}H_{15}$ (**V_6-Ad**), and –$OOCC_9H_{15}N_2OS$ (**V_6-Biot**).

The nucleophilic substitution reactions were performed by mixing **V_6-Cl** with tetrabutylammonium iodide (TBA-I), a carboxylic acid and a base in dry DMA for 2–5 h at 80 °C. Either Na_2CO_3 or tetrabutylammonium hydroxide (TBA-OH) were used as the base and both successfully promoted the nucleophilic substitution reaction. Na_2CO_3 was found to be more suitable for post-functionalization of **V_6-Cl** since hydrolysis of the ester bond after post-functionalization was observed by ESI-MS if the solution was left stirring for too long when

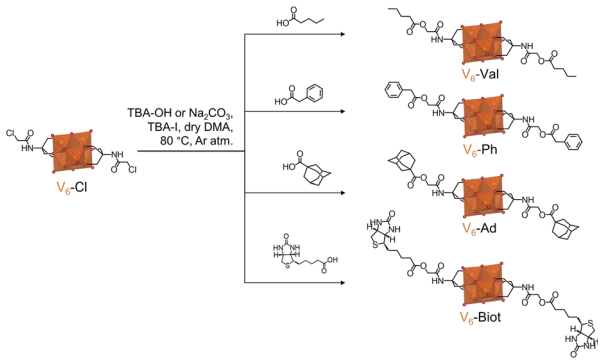

Scheme 3 Post-functionalization of V_6-Cl *via* nucleophilic substitution with valeric acid, phenylacetic acid, adamantanecarboxylic acid, and biotin to form V_6-Val, V_6-Ph, V_6-Ad, and V_6-Biot (top to bottom).

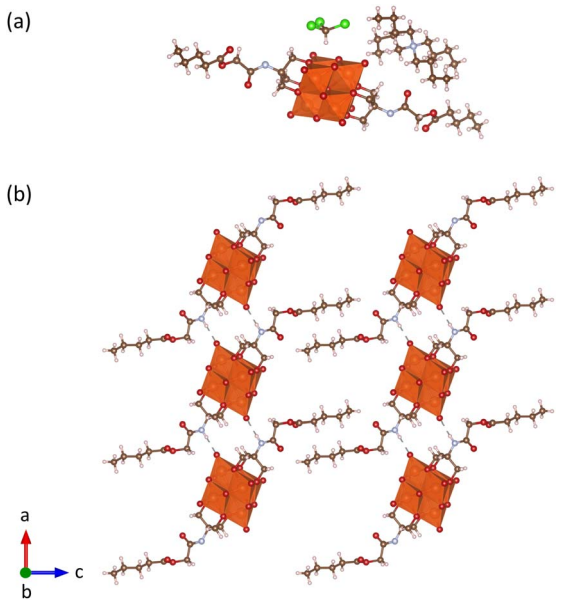

Fig. 5 (a) Structural representation of V_6-Val showcasing the relative position of the $CHCl_3$ and TBA molecules with respect to V_6-Val in the crystal structure (two of each per hexavanadate unit that are symmetrically equivalent). (b) Crystal packing of V_6-Val into a 1D H-bond network (H-bond distances shown as dashed grey lines) viewed along the crystallographic b axis without showing the TBA counter ions and $CHCl_3$ for clarity. Hydrogen in white, carbon in brown, nitrogen in light blue, oxygen in red, chlorine in green and vanadium in orange.

using TBA-OH (Fig. S15–S17†). As a result, the yield and the purity of the product were generally higher with Na_2CO_3 than with TBA-OH. For example, the synthesis of **V_6-Ad** gave a yield of 42% with TBA-OH while with Na_2CO_3 the yield was 50%. Nevertheless, when using Na_2CO_3, a small amount of the Na salt of the HPOM or mixed salts were sometimes obtained, but these could be easily converted back to the desired TBA salt by the addition of excess tetrabutylammonium bromide (TBA-Br). Hence, once the reaction conditions were optimized, post-functionalization of **V_6-Cl** resulted in yields of around 50% or higher overall.

It is worth noting that the post-functionalization of **V_6-Cl** with all selected carboxylic acids was possible despite their differences in steric hindrance and functionality. However, the nature of the organic species being used can have an impact on the outcome of the reaction. This was especially noticeable during the synthesis of **V_6-Ph** since the solution turned green due to the formation of mixed valence **V_6-Ph**. Hence, in order to obtain the desired fully oxidized **V_6-Ph**, an additional oxidation step with H_2O_2 was required. The higher propensity of **V_6-Ph** towards reduction over the other V_6-R HPOMs reported in this study is likely due to the ability of the aromatic ring to transfer electrons to the POM.[56] Additionally, reduction of the V_6 core may be favoured by the stabilising electron-withdrawing inductive effect of the aromatic group.[50,57] This resulted in a slightly lower yield for **V_6-Ph** compared to other V_6-R HPOMs. In contrast, **V_6-Biot** was successfully obtained in relatively high yield, even when using TBA-OH as the base. This is significant because the attempted post-functionalization of V_6-OH with biotin *via* esterification – using *N*,*N*′-dicyclohexylcarbodiimide (DCC) as the coupling agent and 4-dimethylaminopyridine (DMAP) to promote the reaction – was unsuccessful, and the previously reported esterification with stearic acid only gave a relatively low yield (10%).[31] This shows the limitations of V_6-OH as a post-functionalization platform. Furthermore, modifications of the platform to improve its reactivity, such as the incorporation of an alkyne terminal group that has been reported to allow for the attachment of biotin in high yields *via* Huisgen 1,3-cycloaddition, are often not as straightforward as the single-step synthesis of Tris-Cl.[55,58] Therefore, this highlights the versatility and accessibility of **V_6-Cl** for the derivatization of hexavanadates with a wide range of different species to obtain new V_6-R HPOMs in reasonable yields.

Successful post-functionalization of **V_6-Cl** to form and isolate **V_6-Val**, **V_6-Ph**, **V_6-Ad**, and **V_6-Biot** was confirmed by ^{1}H NMR (Fig. S8†) from the disappearance of the peak at around 12 ppm due to the –COOH environment and a downfield shift in the chemical shift of the $-COCH_2-$ group from 4 ppm to around 4.45 ppm due to the chloro (–Cl) functionality being substituted by the carboxylate (–OOC–). The chemical shift and integration of the other peaks in the spectra of each compound were also consistent with the attachment of the carboxylate moieties to both tripodal anchors on the V_6 HPOM (Fig. S8 and S9†). Furthermore, ^{51}V NMR (Fig. S8†) showed that the V_6 POM core structure remained intact after the post-functionalization, giving rise to a single peak at around −495 ppm for all compounds. This was further confirmed from the characteristic peaks at around 700–1000 cm^{-1} in the IR spectra of the compounds due to ν V=O and ν V–O–V vibrations (Fig. S13†). Negative ion mode ESI-MS also showed peaks corresponding to the molecular ions of the POM alone (M^{2-}) or with one TBA counter cation ($[M + TBA]^-$) for each compound. Peaks in positive ion mode due to the POM with extra TBA counter cations ($[M + 3TBA]^+$) were also observed for the POMs with molecular weights within the measurement range. Moreover, the crystal structure of **V_6-Val** (Fig. 5), obtained from crystals formed by slow evaporation of a solution of **V_6-Val** in $CHCl_3$, matched that of **V_6-Cl** with Cl replaced by

the carboxylate. However, unlike **V_6-Cl**, **V_6-Val** crystallized in the monoclinic $P2_1/c$ space group. Yet, **V_6-Val** also formed a 1-D H-bond network due to H-bonding interactions between the –NH group of the amide bond and a terminal oxygen of the hexavanadate POM core with N···O distances of 2.88 Å (Fig. 5(b)). Furthermore, aside from having two TBA molecules per hexavanadate unit as expected, two chloroform molecules per hexavanadate unit were also present in the unit cell (Fig. 5(a)). Overall, this confirms the successful post-functionalization of **V_6-Cl** with carboxylic acids.

Conclusions

In this work, an in-depth investigation of the factors that affect the synthesis of hexavanadates was leveraged to develop **V_6-Cl** as a novel post-functionalization platform. The study showed that the low yields often observed in the synthesis of hexavanadates are linked to the solution properties of the ligand and the reactivity of its functional groups, both of which affect the speciation of vanadates in solution. In general, the formation of a suitable post-functionalization platform requires a ligand with a reactive terminal group, however this may also cause undesired side reactions. Overall, the key factors influencing the synthesis of hybrid hexavanadate clusters were determined to be: (i) the reactivity of the terminal group of the organic ligand with respect to vanadate species in solution, (ii) the solubility of the organic ligand, (iii) the interactions of the solvent with the ligand, which can prevent side reactions, and (iv) the Lewis acidity of the solvent, which affects the ease of reduction of V^{5+}. Controlling these factors was shown to be crucial for the facile, one-step synthesis of **V_6-Cl** in relatively high yields from a decavanadate cluster and Tris-Cl, using DMA as the solvent. We also showed that **V_6-Cl** could be easily post-functionalized with a wide range of carboxylic acids that differ significantly in composition and complexity. The formation of such (bio)organic hybrids with biomolecules, such as biotin, in particular may have potential for the development of antitumor, antiviral, anticancer and anti-amyloid agents,[7,59–62] while adamantane derivatives could be used for drug carrier systems in combination with cyclodextrin, among many other possible applications.[23,61,63–67] Furthermore, this post-functionalization strategy can be extended to functionalization with other organic moieties or even other inorganic clusters, resulting in novel hybrid metal-oxo clusters for potential use in catalysis, medicine and molecular magnetism.[8,10,23,68–70] Hence, through the successful synthesis of **V_6-Cl** as a novel, accessible, and versatile starting point for the formation of various hybrid structures the range of potential applications of polyoxovanadates can be expanded.

Data availability

Crystallographic data for compounds **V_6-Cl** and **V_6-Val** has been deposited at The Cambridge Crystallographic Data Centre (CCDC) and allocated the deposition numbers CCDC 2217991 and 2217992, respectively. All other data supporting the results discussed in this work is available within the paper and its ESI.†

Author contributions

D. E. S. M. and G. K. performed the synthesis and characterisation of all compounds with the assistance of M. A. M. K. V. H. solved the crystal structures. T. N. P.-V. and M. A. M. helped with the design and interpretation of the experiments. The manuscript was written through contributions of all authors. All authors have given approval to the final version of the manuscript.

Conflicts of interest

There are no conflicts to declare.

Acknowledgements

We thank KU Leuven and the Research Foundation Flanders (FWO) for funding. D. E. S. M. (1183021N), G. K. (1185522N) and M. A. M. (1279721N) thank the FWO for PhD and post-doctoral fellowships.

Notes and references

1 C. Sanchez, P. Belleville, M. Popall and L. Nicole, Applications of advanced hybrid organic–inorganic nanomaterials: from laboratory to market, *Chem. Soc. Rev.*, 2011, **40**, 696–753.
2 J. Zhang, Y. Huang, G. Li and Y. Wei, Recent advances in alkoxylation chemistry of polyoxometalates: From synthetic strategies, structural overviews to functional applications, *Coord. Chem. Rev.*, 2019, **378**, 395–414.
3 Y. Zhang, F. de Azambuja and T. N. Parac-Vogt, The forgotten chemistry of group(IV) metals: A survey on the synthesis, structure, and properties of discrete Zr(IV), Hf(IV), and Ti(IV) oxo clusters, *Coord. Chem. Rev.*, 2021, **438**, 213886.
4 S.-S. Wang and G.-Y. Yang, Recent Advances in Polyoxometalate-Catalyzed Reactions, *Chem. Rev.*, 2015, **115**, 4893–4962.
5 Y.-F. Song, *Polyoxometalate-Based Assemblies and Functional Materials*, Springer International Publishing, Cham, 2018, vol. 176.
6 Y. Ji, L. Huang, J. Hu, C. Streb and Y.-F. Song, Polyoxometalate-functionalized nanocarbon materials for energy conversion, energy storage and sensor systems, *Energy Environ. Sci.*, 2015, **8**, 776–789.
7 J. T. Rhule, C. L. Hill, D. A. Judd and R. F. Schinazi, Polyoxometalates in Medicine, *Chem. Rev.*, 1998, **98**, 327–358.
8 M. Stuckart and K. Y. Monakhov, Polyoxometalates as components of supramolecular assemblies, *Chem. Sci.*, 2019, **10**, 4364–4376.
9 A. Proust, R. Thouvenot and P. Gouzerh, Functionalization of polyoxometalates: towards advanced applications in catalysis and materials science, *Chem. Commun.*, 2008, 1837–1852.
10 K. P. Sullivan, W. A. Neiwert, H. Zeng, A. K. Mehta, Q. Yin, D. A. Hillesheim, S. Vivek, P. Yin, D. L. Collins-Wildman,

E. R. Weeks, T. Liu and C. L. Hill, Polyoxometalate-based gelating networks for entrapment and catalytic decontamination, *Chem. Commun.*, 2017, **53**, 11480–11483.

11 Y. Hou, H. An, S. Chang and J. Zhang, Versatile catalysts constructed from hybrid polyoxomolybdates for simultaneously detoxifying sulfur mustard and organophosphate simulants, *Catal. Sci. Technol.*, 2019, **9**, 2445–2455.

12 P. Yin, J. Wang, Z. Xiao, P. Wu, Y. Wei and T. Liu, Polyoxometalate–Organic Hybrid Molecules as Amphiphilic Emulsion Catalysts for Deep Desulfurization, *Chem. – Eur. J.*, 2012, **18**, 9174–9178.

13 M. Anjass, G. A. Lowe and C. Streb, Molecular Vanadium Oxides for Energy Conversion and Energy Storage: Current Trends and Emerging Opportunities, *Angew. Chem., Int. Ed.*, 2021, **60**, 7522–7532.

14 S. Amthor, S. Knoll, M. Heiland, L. Zedler, C. Li, D. Nauroozi, W. Tobaschus, A. K. Mengele, M. Anjass, U. S. Schubert, B. Dietzek-Ivanšić, S. Rau and C. Streb, A photosensitizer–polyoxometalate dyad that enables the decoupling of light and dark reactions for delayed on-demand solar hydrogen production, *Nat. Chem.*, 2022, **14**, 321–327.

15 A. A. Fertig, W. W. Brennessel, J. R. McKone and E. M. Matson, Concerted Multiproton–Multielectron Transfer for the Reduction of O_2 to H_2O with a Polyoxovanadate Cluster, *J. Am. Chem. Soc.*, 2021, **143**, 15756–15768.

16 J. W. Han and C. L. Hill, A Coordination Network That Catalyzes O2-Based Oxidations, *J. Am. Chem. Soc.*, 2007, **129**, 15094–15095.

17 X.-X. Li, Y.-X. Wang, R.-H. Wang, C.-Y. Cui, C.-B. Tian and G.-Y. Yang, Designed Assembly of Heterometallic Cluster Organic Frameworks Based on Anderson-Type Polyoxometalate Clusters, *Angew. Chem., Int. Ed.*, 2016, **55**, 6462–6466.

18 X.-X. Li, L.-J. Zhang, C.-Y. Cui, R.-H. Wang and G.-Y. Yang, Designed Construction of Cluster Organic Frameworks from Lindqvist-type Polyoxovanadate Cluster, *Inorg. Chem.*, 2018, **57**, 10323–10330.

19 H.-R. Tian, Z. Zhang, T.-Y. Dang, S.-M. Liu, Y. Lu and S.-X. Liu, Hollow Lindqvist-like-Shaped {V6} Cluster-Based Metal–Organic Framework for the Highly Efficient Detoxification of Mustard Gas Simulant, *Inorg. Chem.*, 2021, **60**, 840–845.

20 O. Linnenberg, M. Moors, A. Notario-Estévez, X. López, C. de Graaf, S. Peter, C. Baeumer, R. Waser and K. Y. Monakhov, Addressing Multiple Resistive States of Polyoxovanadates: Conductivity as a Function of Individual Molecular Redox States, *J. Am. Chem. Soc.*, 2018, **140**, 16635–16640.

21 L. E. VanGelder, A. M. Kosswattaarachchi, P. L. Forrestel, T. R. Cook and E. M. Matson, Polyoxovanadate-alkoxide clusters as multi-electron charge carriers for symmetric non-aqueous redox flow batteries, *Chem. Sci.*, 2018, **9**, 1692–1699.

22 D. Li, J. Song, P. Yin, S. Simotwo, A. J. Bassler, Y. Aung, J. E. Roberts, K. I. Hardcastle, C. L. Hill and T. Liu, Inorganic-organic hybrid vesicles with counterion- and pH-controlled fluorescent properties, *J. Am. Chem. Soc.*, 2011, **133**, 14010–14016.

23 I. Fa Bamba, C. Falaise, J. Marrot, P. Atheba, G. Gbassi, D. Landy, W. Shepard, M. Haouas and E. Cadot, Host-Guest Complexation Between Cyclodextrins and Hybrid Hexavanadates: What are the Driving Forces?, *Chem. – Eur. J.*, 2021, **27**, 15516–15527.

24 O. Linnenberg, A. Kondinski and K. Y. Monakhov, in *Supramolecular Systems: Chemistry, Types and Applications*, 2017, pp. 39–66.

25 Q. Chen and J. Zubieta, Synthesis and structural characterization of a polyoxovanadate coordination complex with a hexametalate core: $[(n\text{-}C_4H_9)_4N]_2[V_6O_{13}\{O_2NC(CH_2O)_3\}_2]$, *Inorg. Chem.*, 1990, **29**, 1456–1458.

26 B. Hasenknopf, R. Delmont, P. Herson and P. Gouzerh, Anderson-Type Heteropolymolybdates Containing Tris(alkoxo) Ligands: Synthesis and Structural Characterization, *Eur. J. Inorg. Chem.*, 2002, **2002**, 1081–1087.

27 A. V. Anyushin, A. Kondinski and T. N. Parac-Vogt, Hybrid polyoxometalates as post-functionalization platforms: From fundamentals to emerging applications, *Chem. Soc. Rev.*, 2020, **49**, 382–432.

28 B. Huang, Z. Xiao, B. Wu, X. Hu, X. Hu, P. Wu and Y. Wei, Synthesis, crystal structure and spectroscopic studies of a series of hexavanadate hybrids with multiple functional groups, *Inorg. Chem. Front.*, 2017, **4**, 165–170.

29 Q. Chen, D. P. Goshorn, C. P. Scholes, X. L. Tan and J. Zubieta, Coordination compounds of polyoxovanadates with a hexametalate core. Chemical and structural characterization of $[V^V_6O_{13}[(OCH_2)_3CR]_2]_2^-$, $[V^V_6O_{11}(OH)_2[(OCH_2)_3CR]_2]$, $[V^{IV}_4V^V_2O_9(OH)_4[(OCH_2)_3CR]_2]_2^-$, and $[V^{IV}_6O_7(OH)_6](OCH_2)_3CR]_2]_2^-$, *J. Am. Chem. Soc.*, 1992, **114**, 4667–4681.

30 P. Wu, J. Chen, P. Yin, Z. Xiao, J. Zhang, A. Bayaguud and Y. Wei, Solvent-induced supramolecular chirality switching of bis-(trisalkoxy)-hexavanadates, *Polyhedron*, 2013, **52**, 1344–1348.

31 P. Yin, P. Wu, Z. Xiao, D. Li, E. Bitterlich, J. Zhang, P. Cheng, D. V. Vezenov, T. Liu and Y. Wei, A Double-Tailed Fluorescent Surfactant with a Hexavanadate Cluster as the Head Group, *Angew. Chem., Int. Ed.*, 2011, **50**, 2521–2525.

32 P. Wu, Z. Xiao, J. Zhang, J. Hao, J. Chen, P. Yin and Y. Wei, DMAP-catalyzed esterification of pentaerythritol-derivatized POMs: A new route for the functionalization of polyoxometalates, *Chem. Commun.*, 2011, **47**, 5557–5559.

33 A. Bayaguud, K. Chen and Y. Wei, Facile synthesis of an organically-derivatized hexavanadate containing the remote amino group, $TBA_2[V_6O_{13}\{(OCH_2)_3CNH_2\}_2]$, *CrystEngComm*, 2016, **18**, 4042–4045.

34 C. Qin and J. Zubieta, Structural investigations of the hexavanadium core $\{V_6O_{19}\}$ in 'oxidized', mixed valence and 'reduced' clusters of the type $[V^V_{6-n}V^{IV}_nO_{13-n}(OH)_n\{(OCH_2)_3CR\}_2]_2^-$, n=0, 3 and 6, *Inorg. Chim. Acta*, 1992, **198–200**, 95–110.

35 C. P. Pradeep, D.-L. Long, G. N. Newton, Y.-F. Song and L. Cronin, Supramolecular Metal Oxides: Programmed Hierarchical Assembly of a Protein-Sized 21 kDa $[(C_{16}H_{36}N)_{19}\{H_2NC(CH_2O)_3P_2V_3W_{15}O_{59}\}_4]^{5-}$ Polyoxometalate Assembly, *Angew. Chem.*, 2008, **120**, 4460–4463.

36 J. W. Han, K. I. Hardcastle and C. L. Hill, Redox-Active Coordination Polymers from Esterified Hexavanadate Units and Divalent Metal Cations, *Eur. J. Inorg. Chem.*, 2006, **2006**, 2598–2603.

37 C. L. Hill, T. M. Anderson, J. W. Han, D. A. Hillesheim, Y. V. Geletii, N. M. Okun, R. Cao, B. Botar, D. G. Musaev and K. Morokuma, New complexes and materials for O2-based oxidations, *J. Mol. Catal. A: Chem.*, 2006, **251**, 234–238.

38 S. Vanhaecht, T. Quanten and T. N. Parac-Vogt, A Simple Nucleophilic Substitution as a Versatile Postfunctionalization Method for the Coupling of Nucleophiles to an Anderson-Type Polyoxometalate, *Inorg. Chem.*, 2017, **56**, 3095–3101.

39 S. Vanhaecht, J. Jacobs, L. Van Meervelt, T. N. Parac-Vogt, V. Meervelt and T. N. Parac-Vogt, A versatile and highly efficient post-functionalization method for grafting organic molecules onto Anderson-type polyoxometalates, *Dalton Trans.*, 2015, **44**, 19059–19062.

40 S. Vanhaecht, T. Quanten and T. N. Parac-Vogt, A mild post-functionalization method for the vanadium substituted $P_2W_{15}V_3$ Wells-Dawson polyoxometalate based on a copper catalyzed azide-alkyne cycloaddition, *Dalton Trans.*, 2017, **46**, 10215–10219.

41 V. W. Day, W. G. Klemperer and D. J. Maltbie, Where are the protons in $H_3V_{10}O_{28}{}^{3-}$?, *J. Am. Chem. Soc.*, 1987, **109**, 2991–3002.

42 V. W. Day, W. G. Klemperer and O. M. Yaghi, Synthesis and characterization of a soluble oxide inclusion complex, $[CH_3CN.cntnd.(V_{12}O_{32}{}^{4-})]$, *J. Am. Chem. Soc.*, 1989, **111**, 5959–5961.

43 Y. Kikukawa, K. Ogihara and Y. Hayashi, Structure Transformation among Deca-, Dodeca- and Tridecavanadates and Their Properties for Thioanisole Oxidation, *Inorganics*, 2015, **3**, 295–308.

44 D. Rehder, T. Polenova and M. Bühl, *Annu. Rep. NMR Spectrosc.*, 2007, **62**, 49–114.

45 J. M. Missina, L. B. P. Leme, K. Postal, F. S. Santana, D. L. Hughes, E. L. de Sá, R. R. Ribeiro and G. G. Nunes, Accessing decavanadate chemistry with tris(hydroxymethyl) aminomethane, and evaluation of methylene blue bleaching, *Polyhedron*, 2020, **180**, 114414.

46 T. Yamase, Photo- and electrochromism of polyoxometalates and related materials, *Chem. Rev.*, 1998, **98**, 307–325.

47 L. Bi, E. Wang, L. Xu and R. Huang, Synthesis, properties and crystal structure of some polyoxometallates containing the tris(hydroxymethyl)aminomethane cation, *Inorg. Chim. Acta*, 2000, **305**, 163–171.

48 K.-J. Range, R. Zintl and A. M. Heyns, The Thermal Decomposition of Ammonium Metavanadate(V) in Open and Closed Systems, *Z. Für Naturforschung B*, 1988, **43**, 309–317.

49 A. A. Fertig and E. M. Matson, Connecting Thermodynamics and Kinetics of Proton Coupled Electron Transfer at Polyoxovanadate Surfaces Using the Marcus Cross Relation, *Inorg. Chem.*, 2023, **62**, 1958–1967.

50 A. J. Kibler and G. N. Newton, Tuning the electronic structure of organic–inorganic hybrid polyoxometalates: The crucial role of the covalent linkage, *Polyhedron*, 2018, **154**, 1–20.

51 U. Mayer, V. Gutmann and W. Gerger, The acceptor number – A quantitative empirical parameter for the electrophilic properties of solvents, *Monatshefte Für Chem. Chem. Mon.*, 1975, **106**, 1235–1257.

52 B. Keita, D. Bouaziz and L. Nadjo, Solvent Effects on the Redox Potentials of Potassium 12-Tungstosilicate and 18-Tungstodiphosphate, *J. Electrochem. Soc.*, 1988, **135**, 87.

53 S. Ogo, S. Moroi, T. Ueda, K. Komaguchi, S. Hayakawa, Y. Ide, T. Sano and M. Sadakane, Preparation of tetrabutylammonium salt of a mono-Ru(iii)-substituted α-Keggin-type silicotungstate with a 4,4′-bipyridine ligand and its electrochemical behaviour in organic solvents, *Dalton Trans.*, 2013, **42**, 7190–7195.

54 I. Fa Bamba, C. Falaise, G. K. Gbassi, P. Atheba, M. Haouas and E. Cadot, N-tert-butoxycarbonyl (BOC) protected $[V_6O_{13}\{(OCH_2)_3CNH_2\}_2]^{2-}$: synthesis, structural characterization, and solution behavior, *J. Coord. Chem.*, 2020, **73**, 2567–2578.

55 H. Jia, Q. Li, A. Bayaguud, S. She, Y. Huang, K. Chen and Y. Wei, Tosylation of alcohols: an effective strategy for the functional group transformation of organic derivatives of polyoxometalates, *Sci. Rep.*, 2017, **7**, 12523.

56 P. Le Maguerès, S. M. Hubig, S. V. Lindeman, P. Veya and J. K. Kochi, Novel Charge-Transfer Materials via Cocrystallization of Planar Aromatic Donors and Spherical Polyoxometalate Acceptors, *J. Am. Chem. Soc.*, 2000, **122**, 10073–10082.

57 E. V. Anslyn and D. A. Dougherty, *Modern Physical Organic Chemistry*, University Science Books, 2006.

58 O. Linnenberg, A. Kondinski, C. Stöcker and K. Y. Monakhov, The Cu(I)-catalysed Huisgen 1,3-dipolar cycloaddition route to (bio-)organic functionalisation of polyoxovanadates, *Dalton Trans.*, 2017, **46**, 15636–15640.

59 N. Gao, H. Sun, K. Dong, J. Ren, T. Duan, C. Xu and X. Qu, Transition-metal-substituted polyoxometalate derivatives as functional anti-amyloid agents for Alzheimer's disease, *Nat. Commun.*, 2014, **5**, 3422.

60 V. A. Zamolo, G. Modugno, E. Lubian, A. Cazzolaro, F. Mancin, L. Giotta, D. Mastrogiacomo, L. Valli, A. Saccani, S. Krol, M. Bonchio and M. Carraro, Selective Targeting of Proteins by Hybrid Polyoxometalates: Interaction Between a Bis-Biotinylated Hybrid Conjugate and Avidin, *Front. Chem.*, 2018, **6**, 278.

61 Y. Gu, Q. Li, Y. Huang, Y. Zhu, Y. Wei and L. Ruhlmann, Polyoxovanadate-iodobodipy supramolecular assemblies: new agents for high efficiency cancer photochemotherapy, *Chem. Commun.*, 2020, **56**, 2869–2872.

62 S. Park, E. Kim, W. Y. Kim, C. Kang and J. S. Kim, Biotin-guided anticancer drug delivery with acidity-triggered drug release, *Chem. Commun.*, 2015, **51**, 9343–9345.

63 C. Falaise, M. A. Moussawi, S. Floquet, P. A. Abramov, M. N. Sokolov, M. Haouas and E. Cadot, Probing Dynamic Library of Metal-Oxo Building Blocks with γ-Cyclodextrin, *J. Am. Chem. Soc.*, 2018, **140**, 11198–11201.

64 F. Schibilla, J. Voskuhl, N. A. Fokina, J. E. P. Dahl, P. R. Schreiner and B. J. Ravoo, Host–Guest Complexes of Cyclodextrins and Nanodiamonds as a Strong Non-Covalent Binding Motif for Self-Assembled Nanomaterials, *Chem. – Eur. J.*, 2017, **23**, 16059–16065.

65 L. Ni, H. Li, H. Xu, C. Shen, R. Liu, J. Xie, F. Zhang, C. Chen, H. Zhao, T. Zuo and G. Diao, Self-Assembled Supramolecular Polyoxometalate Hybrid Architecture as a Multifunctional Oxidation Catalyst, *ACS Appl. Mater. Interfaces*, 2019, **11**, 38708–38718.

66 A. Štimac, M. Šekutor, K. Mlinarić-Majerski, L. Frkanec and R. Frkanec, Adamantane in Drug Delivery Systems and Surface Recognition, *Mol. Basel Switz.*, 2017, **22**, 297.

67 C. F. Chew, A. Guy and P. C. Biggin, Distribution and Dynamics of Adamantanes in a Lipid Bilayer, *Biophys. J.*, 2008, **95**, 5627–5636.

68 N. Bošnjaković-Pavlović, X. Xu, D. Krstić, J.-M. Gillet, Y. Wei, P. Wu, M. Čolović and A. Spasojević-de Biré, Experimental and theoretical insights of functionalized hexavanadates on Na+/K+-ATPase activity; molecular interaction field, ab initio calculations and in vitro assays, *J. Inorg. Biochem.*, 2019, **198**, 110720.

69 P. Wu, Y. Wang, W. Chen, X. Hu, B. Huang and Z. Xiao, Structural and Magnetical Studies of Mixed-Valence Hexavanadate Hybrids: How Organic Ligands Affect the Magnetism of Polyoxometalates?, *Inorg. Chem.*, 2021, **60**, 4347–4351.

70 D. E. Salazar Marcano, M. A. Moussawi, A. V. Anyushin, S. Lentink, L. Van Meervelt, I. Ivanović-Burmazović and T. N. Parac-Vogt, Versatile post-functionalisation strategy for the formation of modular organic–inorganic polyoxometalate hybrids, *Chem. Sci.*, 2022, **13**, 2891–2899.